Development 138, 2303-2313 (2011) doi:10.1242/dev.060491

Non-cell-autonomous microRNA165 acts in a dose-dependent manner to regulate multiple differentiation status in the *Arabidopsis* root

Shunsuke Miyashima*, Satoshi Koi, Takashi Hashimoto and Keiji Nakajima†

SUMMARY

In the development of multicellular organisms, cell fate is usually determined by exchanging positional information. Animals employ a class of intercellular signaling molecules that specify different cell fates by their dosage, but the existence of an equivalent system has not been demonstrated in plants, except that the growth regulator auxin has been proposed to act in a similar manner in certain developmental contexts. Recently, it has been reported that, in the *Arabidopsis* root meristem, endodermis-derived microRNA (miR) 165/166 non-cell-autonomously suppress the expression of the Class III HD-ZIP transcription factor PHABULOSA (PHB) in the peripheral stele, thereby specifying xylem differentiation. Here, we show that the miR165/166-dependent suppression of *PHB* is required not only for xylem specification, but also for differentiation of the pericycle, as well as for ground tissue patterning. Furthermore, using a plant system that allows quantitative control of miR165 production in the ground tissue, we show that endodermis-derived miR165 acts in a dose-dependent manner to form a graded distribution of *PHB* transcripts across the stele. These results reveal a previously unidentified role of miR165 in the differentiation of a broad range of root cell types and suggest that endodermis-derived miR165 acts in a dose-dependent manner to control multiple differentiation status in the *Arabidopsis* root.

KEY WORDS: *Arabidopsis*, MicroRNA, Patterning, Positional cue, Root

INTRODUCTION

Cell fate determination by positional cues is common to both animal and plant development. In animals, some positional cues activate a particular differentiation program in recipient cells regardless of their concentration, whereas another class of positional cues confer multiple differentiation programs in a dose-dependent manner (Tabata and Takei, 2004). In plant development, few, if any, of the intercellular signaling molecules identified thus far appear to control multiple differentiation status in a dose-dependent manner (Bhalerao and Bennett, 2003; Hara et al., 2007; Stahl et al., 2009; Kondo et al., 2010; Matsuzaki et al., 2010; Sugano et al., 2010).

Owing to its simple structure and amenability to genetic analysis, the *Arabidopsis* root has been used as a model system to study plant tissue patterning. In root cross-sections, different tissue layers are organized in a radially symmetric pattern, with the central stele surrounded by single layers of endodermis, cortex and epidermis (Fig. 1) (Dolan et al., 1993). The endodermis and cortex are together termed the ground tissue. The stele consists of the outermost pericycle layer, which surrounds the inner vascular tissue, in which two xylem cell types, protoxylem and metaxylem, are specified at the peripheral and central positions, respectively, along the single xylem pole (Fig. 1) (Carlsbecker and Helariutta, 2005). Although pattern formation in the *Arabidopsis* root relies on intimate cell-cell communication mediated both by ligand-receptor interactions (Hirakawa et al., 2008; Stahl et al., 2009; Matsuzaki et al., 2010) and mobile transcription factors (Kurata et al., 2005), these molecules generally impart a certain differentiation status to the recipient cells regardless of their dosage. For example, the GRAS-type transcription factor SHORT-ROOT (SHR) moves from the stele to the adjacent cell layer, where it promotes endodermis differentiation and activates the expression of another GRAS-type transcription factor, SCARECROW (SCR), which promotes periclinal cell division (Helariutta et al., 2000; Nakajima et al., 2001; Levesque et al., 2006). Ectopic expression of SHR confers *SCR* expression and endodermis differentiation to the recipient cells (Nakajima et al., 2001; Sena et al., 2004).

Recently, it has been reported that SHR and SCR together activate the transcription of two microRNA (miRNA) genes, *MIR165A* and *MIR166B*, in the endodermis (Carlsbecker et al., 2010). The products of *MIR165A* and *MIR166B*, possibly mature forms of miR165 and miR166, non-cell-autonomously suppress Class III homeodomain leucine zipper (HD-ZIP III) transcripts in the peripheral stele. miRNA-dependent suppression of HD-ZIP III, primarily that of *PHABULOSA* (*PHB*), in the peripheral stele is required for protoxylem differentiation (Carlsbecker et al., 2010). Although that study clearly demonstrated the non-cell-autonomous function of endodermis-derived miR165/166 in repressing HD-ZIP III expression in the stele, it is not yet clear whether this suppression is required solely for the differentiation of protoxylem in the peripheral stele or if it has a broader range of functions in root patterning. Furthermore, it is not known whether miRNA165/166 act simply to eliminate their target transcripts in the peripheral stele or if they act in a dose-dependent manner to define a pattern of target transcript distribution.

Graduate School of Biological Sciences, Nara Institute of Science and Technology, 8916-5 Takayama, Ikoma, Nara 630-0192, Japan.

*Present address: Institute of Biotechnology, University of Helsinki, FIN-00014, Finland
†Author for correspondence (k-nakaji@bs.naist.jp)

Accepted 10 March 2011

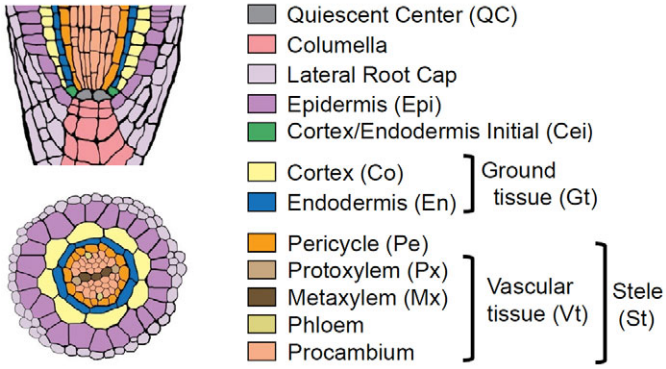

Fig. 1. Tissue organization in the *Arabidopsis* root. Longitudinal (top) and transverse (bottom) sections of the meristematic region of the *Arabidopsis* root. The tissue labels used in subsequent figures are defined.

In this study, we first addressed the role of miR165/166-dependent suppression of PHB in ground tissue patterning and pericycle differentiation, and then analyzed the means by which ground tissue-derived miR165 regulates the *PHB* expression pattern in the stele. Analyses in an inducible miR165 expression line revealed that ground tissue-derived miR165 acts in a dose-dependent manner to establish a PHB expression gradient across the stele, which in turn is required for the correct differentiation of two xylem cell types and the pericycle.

MATERIALS AND METHODS

Plant materials, growth conditions and gene identity

Arabidopsis mutant/marker lines are listed in Table 1. AGI codes for the genes described in this study are as follows: *ACT7*, At5g09810; *AHP6*, At1g80100; *ATHB8*, At4g32880; *AGO1*, At1g48410; *CNA*, At1g52150; *CRE1*, At2g01830; *JKD*, At5g03510; *MIR165A*, At1g01183; *MIR165B*, At4g00885; *MIR166A*, At2g46685; *MIR166B*, At3g61897; *MIR166C*, At5g08712; *MIR166D*, At5g08717; *MIR166E*, At5g41905; *MIR166F*, At5g43603; *MIR166G*, At5g63715; *PHB*, At2g34710; *PHV*, At1g30490; *REV*, At5g60690; *SCR*, At3g54220; *SHR*, At4g37650; and *SKOR*, At3g02850. Because all *Arabidopsis* lines had the Col background except for *phb-1d* (in L*er*) (McConnell and Barton, 1998), *phb-1d* was crossed twice with Col-0 to reduce possible phenotypic differences between the two ecotypes, and heterozygous *phb-1d*/+ plants were used throughout the study. Plant growth conditions were as described (Miyashima et al., 2009).

Expression analysis

For quantitative real-time RT-PCR (qRT-PCR), RNA was extracted from the root meristem region (the distal ~1 cm of the root tip) using the RNeasy Plant Mini Kit (Qiagen, Valencia, CA, USA), and reverse-transcribed using Super Script II reverse transcriptase (Invitrogen, Carlsbad, CA) with oligo(dT) primers (Invitrogen). qRT-PCR was performed using Cyber Premix ExTaq (Takara Bio, Shiga, Japan) and the Light Cycler System (Roche Diagnostics, Basel, Switzerland). Expression levels were normalized to that of *ACTIN 7* (*ACT7*). For the measurement of mature miR165/166, pulsed reverse transcription (Tang et al., 2006) was performed with oligo(dT) and miR165UPL primers. The primers used are listed in Table S1 in the supplementary material.

RNA in situ hybridization

Excised roots were fixed with 4% (w/v) paraformaldehyde in phosphate-buffered saline (PBS, pH 7.0) for 12 hours at 4°C, dehydrated in ethyl and a tertiary butyl alcohol series and embedded in Paraplast Plus (McCormick Scientific, St Louis, MO, USA). Sections (6-8 μm) were mounted on MAS-coated glass slides (Matsunami Glass, Osaka, Japan). For preparation of the *PHB* riboprobe, 936 bp PHB coding sequence was amplified by RT-PCR from Col-0 root RNA with the primers listed in Table S1 in the supplementary material, and cloned into the pGEM-T vector (Promega, Madison, WI, USA). The *PHB* riboprobe was transcribed with the DIG RNA Labeling Kit (Roche Diagnostics) and partially hydrolyzed to ~300 bp. In situ hybridization was performed as described (Kouchi and Hata, 1993). Signals were detected with the DIG Nucleic Acid Detection Kit (Roche Diagnostics).

DNA construction and the generation of transgenic plants

Primers used for DNA construction are listed in Table S1 in the supplementary material. For the construction of endoplasmic reticulum (ER)-localized GFP reporters for *MIR165/166*, *JKD* and *SKOR* (*pMIR165/166-GFPer*, *pJKD-GFPer* and *pSKOR-GFPer*), the 5′ upstream region of each gene was amplified by PCR and fused with the GFPer coding region kindly provided by Jim Haseloff (Cambridge, UK).

For the construction of *PHB-GFP* and *PHBmu-GFP*, an 8.5 kb *PHB* genomic fragment including 3.6 kb promoter and 0.6 kb 3′ regions was amplified from Col-0 genomic DNA with primers Xba-PHB-(–)3570 and Kpn-PHB-(+)5015R, digested with *Xba*I and *Kpn*I, and cloned into the pAN19 vector (modified pUC19) to produce pAN-PHB. miRNA-resistant mutations were introduced by inverse PCR amplification of pAN-PHB with primers PHB(+)miR1445F and PHB(+)miR1444R, followed by self-ligation to produce pAN-PHBmu. In order to insert a GFP coding sequence at the C-termini of the PHB and PHBmu coding regions, a 1.1 kb *Bgl*II-*Kpn*I fragment spanning the C-terminal coding region and the 0.6 kb 3′ region of *PHB* was excised from pAN-PHB and cloned into pAN19 to produce pAN-PHB-Cter. A *Hpa*I restriction site was created immediately before the *PHB* stop codon of pAN-PHB-Cter by inverse PCR amplification with primers HpaI-PHBCterF and PHB(+)4443R, followed by self-ligation. A blunt-ended 3xGly-GFP(S65T) coding sequence (Morita et al., 2002) was inserted at the *Hpa*I site of pAN-PHB-Cter to produce pAN-PHB-Cter-GFP. A *Bgl*II-*Kpn*I fragment containing PHB-Cter-GFP-PHB-3′ was used to replace the corresponding regions of pAN-PHB and pAN-PHBmu to give pAN-PHB-GFP and pAN-PHBmu-GFP, respectively. Finally, the PHB-GFP and PHBmu-GFP fragments were inserted into pBIN30 (modified pBIN19 with Basta resistance).

Table 1. Plant materials

Mutant or line	Background	ABRC stock	Reference
scr-3/sgr1-1	Col-0	CS3997	Fukaki et al., 1998
scr-5	Col-0	–	Paquette and Benfey, 2005
shr-2/sgr7-1	*gl1*/Col-0	CS2972	Fukaki et al., 1998
phb-1d	L*er*	CS3761	McConnell and Barton, 1998
pSCR-SHR	Col-0	–	Nakajima et al., 2001
pSHR-SHR-GFP	*shr-2*/Col-0	–	Nakajima et al., 2001
pSCR-GFP-SCR	*scr-3*/Col-0	–	Gallagher et al., 2004
pAHP6-GFPer	Col-0	–	Mähönen et al., 2006
pPHB-GFPer	Col-0	–	Lee et al., 2006
pCRE1-MIR165A	Col-0	–	Carlsbecker et al., 2010

ABRC, Arabidopsis Biological Resource Center.

For the construction of *MIR165Amu*, a 4.6 kb *MIR165A* genomic fragment including 3.9 kb promoter and 0.6 kb 3′ regions was amplified from Col-0 genomic DNA by PCR with primers miR165a(–)3927 and miR165a(+)722R and cloned into the pAN19 vector to give pAN-MIR165A. Mutations enabling miR165 to suppress *PHBmu* were introduced in the same way as for *PHBmu-GFP* described above, with primers miR165a(+)93mu and miR165a(+)70R. The *MIR165Amu* fragment was then inserted into the pBIN40 binary vector (modified pBIN19 with hygromycin resistance).

The *pJ0571-GVG UAS-tdTomatoEr UAS-PHBmu-GFP* transgenic plants were generated by sequentially transforming *Arabidopsis* plants with the *pJ0571-GVG UAS-tdTomatoEr* and *UAS-PHBmu-GFP* constructs. For construction of *pJ0571-GVG UAS-tdTomatoEr*, the T-DNA insertion site in the enhancer trap line *J0571* (Jim Haseloff) was identified between At4g39900 and At4g39910 by TAIL-PCR (Liu et al., 1995) and subsequent co-segregation analysis. A 0.8 kb ground tissue-specific enhancer sequence (*pJ0571*) was amplified from *J0571* genomic DNA with the primers listed in Table S1 in the supplementary material. The GAL4:VP16:GR (GVG) coding sequence was constructed by fusing the GAL4:VP16 (GV) coding region amplified from an enhancer trap line (Jim Haseloff) with the rat GR coding sequence (Lloyd et al., 1994). tdTomatoEr coding sequence was generated by fusing a signal peptide (MKTNLFLFLIFSLLLSLSSAEL) and ER-retention signal (HDEL) sequences to the 5′ and 3′ ends, respectively, of the tdTomato coding sequence (Shaner et al., 2004). The tdTomatoEr coding sequence was then inserted between the *5xUAS-TATA* (gift from Jim Haseloff) and the nopaline synthase terminator (NosT) to produce *UAS-tdTomatoEr-NosT*. The resulting *pJ0571-GVG* and *UAS-tdTomatoEr-NosT* were assembled in the pBIN19 vector. For *UAS-PHBmu-GFP* construction, a DNA fragment containing the PHBmu-GFP coding region was amplified from pAN-PHBmu-GFP with primers PHB(–)287 and PHB-4546R, and inserted between the *5xUAS-TATA* and NosT in the pBIB vector (Becker, 1990).

The *indMIR165Amu/PHBmu-GFP* plants (genotype *pJ0571-GVG UAS-tdTomatoEr UAS-MIR165Amu PHBmu-GFP*) were obtained by crossing plants harboring the *pJ0571-GVG UAS-tdTomatoEr UAS-MIR165Amu* with plants homozygous for *PHBmu-GFP* and heterozygous for *MIR165Amu*, and maintained as a line heterozygous for *MIR165Amu* and homozygous for the other transgenes. Progeny lacking *MIR165Amu* can be easily identified by their *phb-1d*-like appearance and were used for transcriptional activation experiments. For the construction of *pJ0571-GVG UAS-tdTomatoEr UAS-MIR165Amu*, the *MIR165Amu* transcribed regions were amplified with primers Hind-MIR165A(–)33 and Bam-MIR165A(+)135R and inserted between *5xUAS-TATA* and NosT. The resulting *UAS-MIR165Amu-NosT* fragment was inserted into the vector containing *pJ0571-GVG* and *UAS-tdTomatoEr* described above. The control *indMIR165A/PHBmu-GFP* plants (expressing wild-type miR165, genotype *pJ0571-GVG UAS-tdTomatoEr UAS-MIR165A PHBmu-GFP*) were generated similarly using a construct harboring *MIR165A*.

pCRE1-MIR165A and *pAHP6-GFPer* were gifts from Yka Helariutta (University of Helsinki, Finland) and *pPHB-GFPer* was a gift from Ji-Young Lee (Cornell University, NY, USA).

All binary plasmids were introduced into *Agrobacterium tumefaciens* strain GV3-101 and used to transform *Arabidopsis* plants by floral dip (Clough and Bent, 1998).

Histological analysis and microscopy

Confocal laser-scanning microscopy (CLSM) and preparation of root cross-sections were carried out as described (Miyashima et al., 2009). Fluorescence intensity was measured with ImageJ (NIH) and LAS AF (Leica Microsystems, Wetzlar, Germany) software. For auxin treatment, seeds were germinated on agar media containing 10 μM *N*-1-naphthylphthalamic acid (NPA). Three days post-germination, seedlings were transferred to agar media containing 10 μM naphthalene acetic acid (NAA), grown for 20 hours and then observed by differential interference contrast (DIC) microscopy with a Nikon E1000 microscope (Nikon, Tokyo, Japan) after tissue clearing with 8:1:1 (w:v:v) chloral hydrate:glycerol:water. The xylem cell wall was visualized by Safranin (Kubo et al., 2005) or propidium iodide staining followed by CLSM or DIC microscopy after tissue clearing. Lateral root primordia were also observed by DIC microscopy after tissue clearing.

Microarray analysis

RNA samples were prepared from Col-0, *scr-3* and *ago1-101* roots (Miyashima et al., 2009) as described above. Two-color microarray hybridization was performed for the pairs *scr-3*/Col and *ago1-101*/Col using a 44K Arabidopsis 3 microarray (Agilent Technologies, Palo Alto, CA, USA). Dye-swap replication was performed for each experiment. Microarray data have been deposited at GEO with accession number GSE16460.

RESULTS

miRNA-dependent suppression of *PHB* is required for ground tissue patterning

Loss-of-function *argonaute 1* (*ago1*) mutants exhibit root radial pattern defects in the ground tissue (Miyashima et al., 2009). In a search for *ago1*-dependent genes in the *Arabidopsis* root by microarray analysis, we found that three HD-ZIP III genes, *PHB*, *PHAVOLUTA* (*PHV*) and *REVOLUTA* (*REV*), were upregulated in *ago1* (see Fig. S1 in the supplementary material). Expression of HD-ZIP III genes is suppressed by the action of miR165 and miR166 (McConnell et al., 2001; Prigge et al., 2005; Ochando et al., 2008). To examine whether the radial pattern defects of *ago1* roots were caused by upregulation of HD-ZIP III genes, we analyzed the root radial pattern of a dominant *phb-1d* mutant that expresses miRNA-resistant *PHB* transcripts as a result of an insertion in its miR165/166 target site (McConnell et al., 2001; Mallory et al., 2004). Serial cross-sections from the root meristem region revealed that the *phb-1d* stele is composed of fewer cell files (25.3±3.7, n=8) than wild-type stele (50.1±3.1, n=8), and that most (9 of 11) *phb-1d* roots contained an extra layer in one or two cortex cell files (compare Fig. 2A with 2B).

Because the number of root ground tissue layers is controlled by the actions of SHR and its downstream target SCR (Nakajima et al., 2001; Levesque et al., 2006; Cui et al., 2007), we analyzed the distribution of SHR:GFP and GFP:SCR fusion proteins in *phb-1d*. In wild-type roots, SHR:GFP is localized to both the cytoplasm and nucleus of the stele, the site of their synthesis (Nakajima et al., 2001). SHR:GFP is also detected in a single layer adjacent to the stele, where it is localized exclusively to the nucleus, and no GFP fluorescence is detected in external cell layers (Fig. 2C) (Nakajima et al., 2001). GFP:SCR is localized exclusively to the nucleus of the single layer adjacent to the stele (Fig. 2D) (Gallagher et al., 2004). In *phb-1d* roots, nuclear-localized SHR:GFP and GFP:SCR were detected not only in a single cell layer adjacent to the stele, but also in the supernumerary ground tissue layers (arrows in Fig. 2E,F).

It has been reported that loss-of-function mutations in a putative zinc-finger transcription factor gene, *JACKDAW* (*JKD*), result in patches of supernumerary ground tissue layers owing to unrestricted intercellular movement of SHR towards the cortex (Welch et al., 2007). Consistent with this report, expression of a *pJKD-GFPer* reporter and the level of endogenous *JKD* transcripts measured by qRT-PCR were reduced in *phb-1d* (Fig. 2G-I). Quantification of GFP fluorescence intensity indicated that the downregulation of *JKD* is more pronounced in the ground tissue than in the quiescent center (QC) (Fig. 2J), suggesting that the moderate decrease in the *JKD* transcript level measured in root extracts was due to selective downregulation of *JKD* in the *phb-1d* ground tissue or to the severe reduction in the number of stele cell files, which increases the proportion of ground tissue-derived RNA

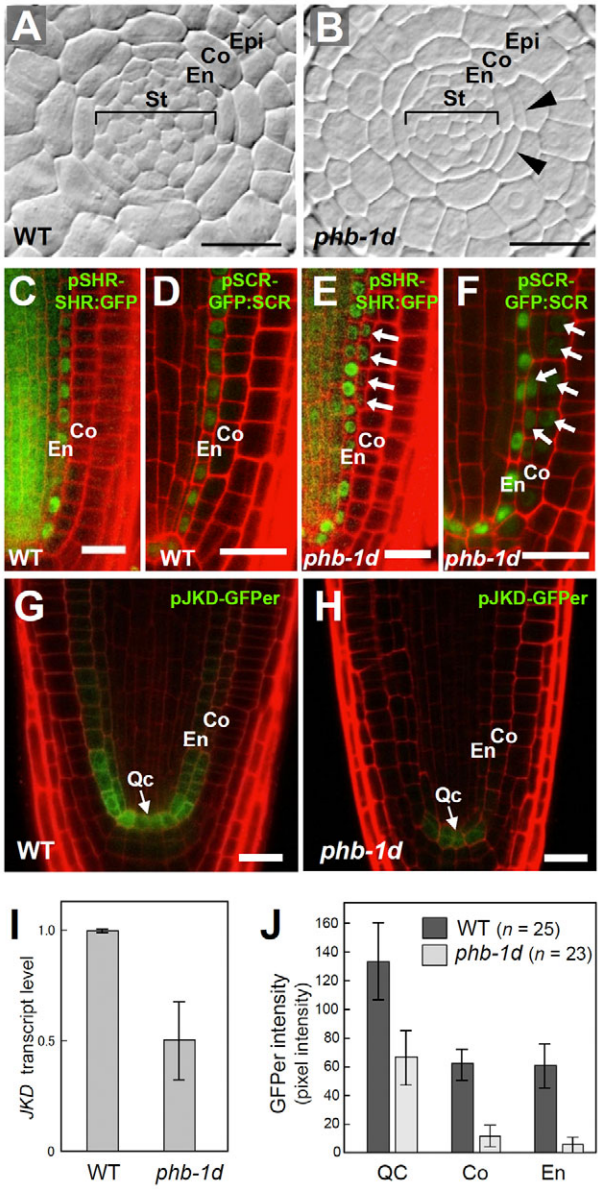

Fig. 2. *phb-1d* roots are defective in ground tissue patterning. (**A**,**B**) Transverse sections of wild-type (WT, A) and *phb-1d* (B) *Arabidopsis* roots. Arrowheads indicate ectopic periclinal division of *phb-1d* ground tissue. (**C-F**) Expression of GFP-tagged SHR (C,E) and SCR (D,F) in wild-type (C,D) and *phb-1d* (E,F) roots. Arrows indicate GFP-tagged SHR and SCR detected outside the endodermis in *phb-1d*. (**G**,**H**) Expression of *pJKD-GFPer* in wild-type (G) and *phb-1d* (H) roots. *JKD* transcription is attenuated in *phb-1d*. (**I**) *JKD* transcript levels in wild-type and *phb-1d* roots as measured by qRT-PCR. (**J**) *pJKD-GFPer* fluorescence intensity in the quiescent center, cortex and endodermis in wild-type and *phb-1d* backgrounds. Error bars represent s.d. from three replicates. Scale bars: 20 μm.

in whole root extracts. These results suggest that miRNA-dependent suppression of *PHB* is required to maintain *JKD* expression in the ground tissue, which in turn regulates ground tissue patterning by restricting SHR and SCR proteins to the endodermis.

miRNA-dependent suppression of *PHB* is required for pericycle differentiation

Specification of xylem cell types is controlled by the dosage of HD-ZIP III activities: a high dosage specifies metaxylem and a low dosage specifies protoxylem (Carlsbecker et al., 2010). HD-ZIP III activity in the peripheral stele is suppressed by the miR165/166 derived from the endodermis, which in turn is controlled by SHR- and SCR-dependent transcription. As a result, ectopic metaxylem is formed at the protoxylem position in *phb-1d*, *scr-3* and *shr-2*, where the *PHB* expression domain is expanded (Carlsbecker et al., 2010) (see Fig. S2 in the supplementary material). To examine whether the expansion of the *PHB* expression domain affects other cell types in the root stele, we analyzed the differentiation status of the pericycle in these mutants.

We examined our microarray data, comparing the transcript profiles of *scr-3* and wild type, as well as the previously published expression map of the *Arabidopsis* root meristem (Birnbaum et al., 2003). We found that several genes known to function in the root stele were downregulated in *scr-3* (see Table S2 in the supplementary material). *ARABIDOPSIS HISTIDINE PHOSPHOTRANSFER PROTEIN 6* (*AHP6*) is expressed in the protoxylem precursors and abutting pericycle cells (Mähönen et al., 2006). In order to visualize the expression pattern of *AHP6*, we introduced the *pAHP6-GFPer* reporter (Mähönen et al., 2006) into *scr-3* and *phb-1d*. In wild-type root, *AHP6* is expressed in a pair of three-cell domains comprising one protoxylem and two abutting pericycle cells (Fig. 3A) (Mähönen et al., 2006). In *phb-1d* roots, *AHP6* expression was lost completely or detected in only one cell of the three (88.5%, *n*=26; Fig. 3B). In *scr-3*, *AHP6* expression was lost in the pericycle cells and expression attenuated in the protoxylem (100%, *n*=10; Fig. 3C). We also generated a *GFPer* reporter for the *STELAR* K^+ *OUTWARD RECTIFIER* (*SKOR*) gene involved in the release of potassium to the xylem sap (*pSKOR-GFPer*) (Gaymard et al., 1998). *SKOR* is normally expressed in the pericycle, near the xylem pole and above the differentiation zone (Fig. 3D,G). In both *phb-1d* and *scr-3*, *SKOR* expression was severely reduced, indicating that pericycle function is at least partly affected in these mutants (Fig. 3E,F,H,I). Aberrant function of the pericycle in *scr-3* and *phb-1d* was also suggested by reduced periclinal division in response to external auxin (Himanen et al., 2002; Fukaki and Tasaka, 2009) (Fig. 3J-L). These results indicate that miRNA-dependent suppression of *PHB* is required not only for protoxylem specification, but also for the correct differentiation of the pericycle.

Three *MIR165/166* genes are transcribed in the endodermis

The *Arabidopsis* genome contains nine *MIR165/166* genes (*MIR165A*, *MIR165B* and *MIR166A-G*) that potentially regulate the expression of the HD-ZIP III genes including *PHB* (Reinhart et al., 2002; Tang et al., 2003). Carlsbecker et al. analyzed the expression of eight *MIR165/166* genes (all but *MIR165B*) and found that *MIR165A* and *MIR166B* are expressed specifically in the root endodermis in an *SHR*- and *SCR*-dependent manner (Carlsbecker et al., 2010). We independently constructed GFPer reporters for all nine *MIR165/166* genes and found that, in addition to *MIR165A* and *MIR166B*, *MIR166A* is also expressed in the endodermis (see Fig. S3A,D,G,J-L in the supplementary material). Our reporter analysis also suggested that *MIR166A* and *MIR166B* are expressed in the QC (see Fig. S3D,G in the supplementary material). Similar to *MIR165A* and *MIR166B*, expression of *MIR166A* was also dependent on *SCR* (see Fig. S3B,E,H in the supplementary

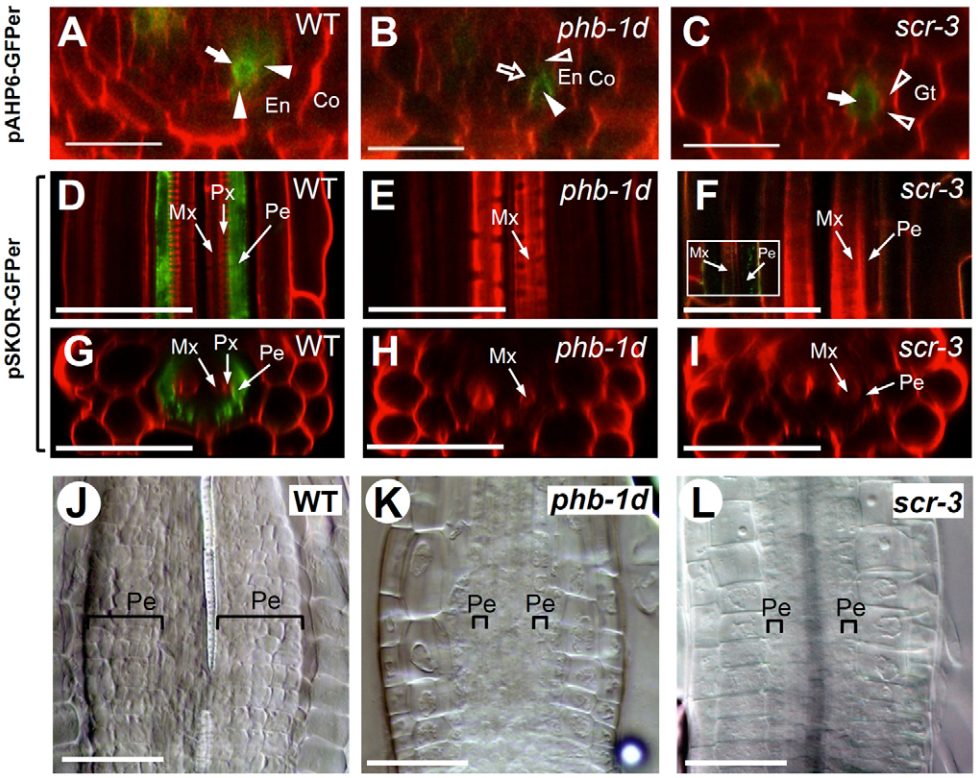

Fig. 3. *phb-1d* and *scr-3* roots are defective in pericycle differentiation. (**A-C**) Confocal images showing the expression pattern of *pAHP6-GFPer*. In wild-type *Arabidopsis* roots (A), *pAHP6-GFPer* is expressed in a protoxylem cell file (solid arrow) and two abutting pericycle cell files (solid arrowheads). In *phb-1d* (B) and *scr-3* (C), *pAHP6-GFPer* expression is either attenuated or lost in some of the cell files (open arrows and arrowheads). (**D-I**) Confocal images showing the expression pattern of *pSKOR-GFPer*. In wild type (D,G), *pSKOR-GFPer* is expressed in pericycle cell files preferentially toward the xylem pole. In *phb-1d* (E,H) and *scr-3* (F,L), expression of *pSKOR-GFPer* is barely detectable. Inset in F shows weak GFP signal in the *scr-3* pericycle as visualized at higher detector sensitivity. (**J-L**) Effect of exogenous auxin on the periclinal division of root pericycle. Wild-type root shows massive proliferation of pericycle cells upon NPA/NAA treatment (J), whereas *phb-1d* (K) and *scr-3* (L) root pericycle respond poorly to the same treatment. Brackets indicate pericycle layers. Scale bars: 50 μm.

material). The extent of the *SCR* dependence varied among the three *MIR165/166* genes: with increased detector sensitivity, considerable expression of the GFPer reporter was detected for *MIR166B*, whereas it was barely detectable for *MIR165A* and *MIR166A* (see Fig. S3C,F,I in the supplementary material). Consistent with these observations, total levels of mature miR165/166 were reduced to 20-40% of wild-type levels in *scr* and *shr* mutants (see Fig. S3M in the supplementary material). *SHR*- and *SCR*-dependent expression of the three *MIR165/166* genes was also confirmed by introducing each reporter line into a *pSCR-SHR* background. GFPer fluorescence was detected throughout the supernumerary ground tissue layers, where both *SHR* and *SCR* are expressed (see Fig. S4 in the supplementary material) (Nakajima et al., 2001). These results indicate that the single cell layer, composed of the endodermis and QC, acts as the sole source of miR165/166 in the *Arabidopsis* root meristem.

Transgenic *PHB-GFP* and *PHBmu-GFP* lines closely mimic the endogenous *PHB* expression pattern and miR-resistant *phb* mutant phenotype

To correlate the *PHB* expression pattern and the level of miR165/166 in the endodermis, we generated reporter lines for *PHB* expression (*PHB-GFP*) in which the GFP coding sequence was inserted into the genomic context of *PHB* (Fig. 4A). In the wild-type background, PHB:GFP showed a graded expression pattern in the stele, with a peak at the center and gradually decreasing toward the periphery (Fig. 4B). Introduction of silent mutations into the miR165/166 target site of *PHB-GFP* (Mallory et al., 2004) (*PHBmu-GFP*) resulted in GFP fluorescence that was distributed throughout all cell layers (Fig. 4C), with nearly uniform intensity across the stele (compare bottom panels of Fig. 4B,C). This expression pattern of PHBmu:GFP is likely to reflect the transcription pattern of *PHB*, as a *pPHB-GFPer* transcriptional reporter showed a similar distribution of GFPer fluorescence to *PHBmu-GFP* (see Fig. S5 in the supplementary material) (Lee et al., 2006).

We then crossed the *PHB-GFP* reporter line with *scr-3*. In *scr-3*, PHB:GFP still showed a graded distribution pattern, as in wild type, but its expression domain was expanded to include the whole stele (Fig. 4D). The expression pattern of PHB:GFP in *shr-2* was very similar to that in *scr-3* (Fig. 4F). This expression pattern was somewhat intermediary between those of *PHB-GFP* and *PHBmu-GFP* (compare Fig. 4B-D,F), and consistent with the observation that expression of miR165/166 in the endodermis is reduced in *scr-3* and *shr-2*, but not totally abolished (see Fig. S3I,M in the supplementary material).

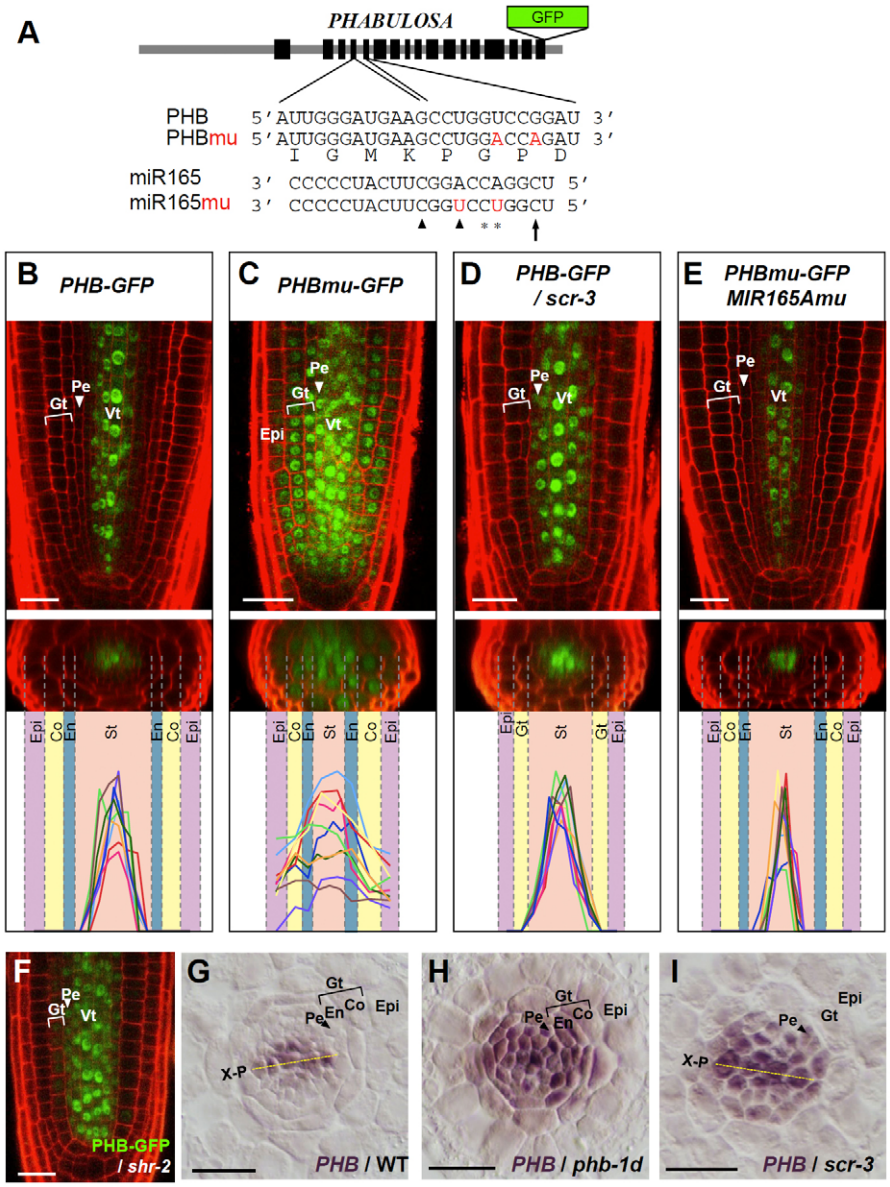

Fig. 4. *PHB-GFP* and *PHBmu-GFP* markers faithfully report the expression patterns of endogenous *PHB* and its miRNA-resistant transcripts, respectively. (**A**) Nucleotide sequences of miR165 and its target site in *PHB*. Mutations introduced into *PHBmu-GFP* and miR165mu are in red. Among the two mutations introduced into miR165mu, one at the 5′ side was to recover complementarity to *PHBmu*, whereas the other at the 3′ side was to retain the same number of mismatches (two) between *PHBmu* and miR165mu as between *PHBmu* and miR165. Certain positions are marked on miR165 according to their contribution to *PHB* repression (Mallory et al., 2004); asterisks, strong effects; arrowheads, weak effects; arrow, no effect. (**B-F**) Expression patterns of *PHB-GFP* and *PHBmu-GFP* in various genetic backgrounds. Graphs beneath B-E show GFP signal intensity (arbitrary units) measured across the root diameter for ten roots for each line. (**G-I**) In situ hybridization of root transverse sections with a *PHB* antisense probe. X-P, xylem pole. Note that expression patterns of *PHB-GFP* in wild type (A) and *scr-3* (C) correlate well with the patterns of *PHB* transcript accumulation in each genotype (G,I). Expression of *PHBmu-GFP* (C) is similar to the *phb-1d* transcript pattern (H), whereas co-expression of *PHBmu-GFP* and *MIR165Amu* (E) makes it indistinguishable from the expression pattern of *PHB-GFP* in wild-type root (B). Scale bars: 20 μm.

The fidelity of the *PHB-GFP* and *PHBmu-GFP* reporters in monitoring the expression patterns and functions of endogenous *PHB* was confirmed by three experiments. First, in situ hybridization revealed the same distribution patterns of endogenous *PHB* transcripts as those of PHB:GFP and PHBmu:GFP proteins in wild type and *phb-1d*, respectively (compare Fig. 4B with 4G and Fig. 4C with 4H). The expression pattern of PHB:GFP in *scr-3* was also consistent with the distribution of endogenous *PHB* transcripts in *scr-3* (compare Fig. 4D with 4I). Second, transcription of *PHBmu-GFP* by the ground tissue-specific *J0571* promoter resulted in the expression of PHBmu:GFP protein exclusively in the ground tissue, indicating that PHBmu:GFP (which is identical to PHB:GFP in amino acid sequence) does not move from the sites of its production (see Fig. S6 in the supplementary material). Third, *PHBmu-GFP* plants were indistinguishable from strong *phb-1d* mutants in every morphological aspect: both *phb-1d* and *PHBmu-GFP* bore narrow cotyledons and filamentous leaves due to the loss of abaxial-adaxial polarity (see Fig. S7A,C in the supplementary material) (McConnell and Barton, 1998; McConnell et al., 2001). They both had supernumerary ground tissue layers in roots (see Fig. S7B,D in the supplementary material). Most notably, *PHBmu-GFP* roots had the same cell differentiation defects in the stele as observed for *phb-1d*, with metaxylem formed with the expense of protoxylem (see Fig. S2B,E,I in the supplementary material), and the expression of *pSKOR-GFPer* was severely attenuated in *PHBmu-GFP* roots (see Fig. S7G in the supplementary material). All these observations indicate that the expression patterns and phenotypes obtained from the *PHB-GFP* and *PHBmu-GFP* reporter lines reflect the endogenous *PHB* expression pattern and the morphological defects caused by the loss of miRNA-dependent suppression.

Endodermis-derived miR165 restricts the PHB expression domain and cell differentiation within the stele in a dose-dependent manner

To visualize the efficiency of PHB suppression by endodermis-derived miR165 outside the endodermis, we constructed a mutated *MIR165A* gene, the product of which targets *PHBmu-GFP*

transcripts, in the context of the genomic *MIR165A* sequence including its own promoter (hereafter *MIR165Amu* for the transgene and miR165mu for its mature miRNA product) (Fig. 4A), and co-expressed it with the *PHBmu-GFP* reporter. In the presence of *MIR165Amu*, the distribution pattern of PHBmu:GFP became indistinguishable from that of the miRNA-sensitive PHB:GFP in wild-type roots (compare Fig. 4B with 4E). Moreover, *MIR165Amu* rescued all morphological defects caused by the *PHBmu-GFP* transgene (see Fig. S7E,F in the supplementary material), as well as protoxylem differentiation (see Fig. S2E,F,I in the supplementary material) and *pSKOR-GFPer* expression (see Fig. S7H in the supplementary material). These results indicate that miR165mu produced in the endodermis allows *PHBmu-GFP* transcripts to recapitulate the wild-type distribution pattern of *PHB*, and that the *PHBmu-GFP* and *MIR165Amu* transgenes closely mimic the relationship between the endogenous *PHB* and *MIR165A* genes.

Having confirmed the reliability of *PHBmu-GFP* and miR165mu in reporting the interaction between endogenous *PHB* and miR165, we modified this system to address quantitative aspects of the capacity of ground tissue-derived miR165 to suppress *PHB* and cell differentiation in the stele. The transcribed region of *MIR165Amu* was placed downstream of the binding site for the steroid hormone-inducible GVG transcriptional activator (Aoyama and Chua, 1997), and the resulting gene, *UAS-MIR165Amu*, was assembled with the

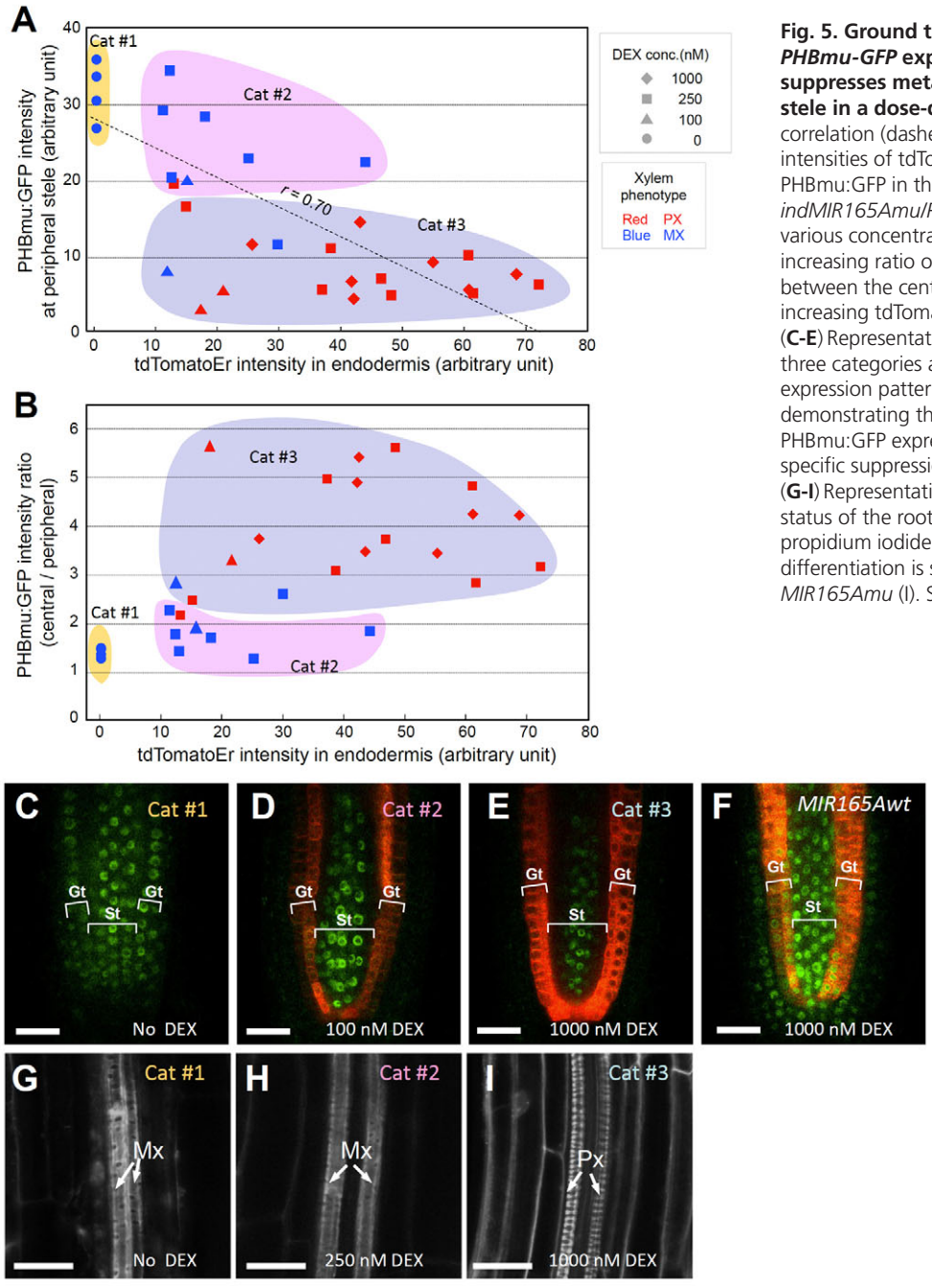

Fig. 5. Ground tissue-derived mi165mu restricts *PHBmu-GFP* expression to the central stele and suppresses metaxylem formation at the peripheral stele in a dose-dependent manner. (**A**) The inverse correlation (dashed line) between the fluorescence intensities of tdTomatoEr in the endodermis and PHBmu:GFP in the peripheral stele of individual *indMIR165Amu/PHBmu-GFP Arabidopsis* roots grown with various concentrations of dexamethasone (DEX). (**B**) The increasing ratio of PHBmu:GFP fluorescence intensity between the central and peripheral stele in response to the increasing tdTomatoEr intensity in the endodermis. (**C-E**) Representative confocal images of the roots of the three categories as classified by their PHBmu:GFP expression patterns (see main text). (**F**) Control experiment demonstrating the inability of wild-type miR165 to affect PHBmu:GFP expression, indicating a highly sequence-specific suppression of PHBmu:GFP by miR165mu. (**G-I**) Representative images of the xylem differentiation status of the roots in the three categories as visualized by propidium iodide staining. Note that ectopic metaxylem differentiation is suppressed only with strong induction of *MIR165Amu* (I). Scale bars: 25 μm.

ground tissue-specific *pJ0571-GVG* driver and the *UAS-tdTomatoEr* reporter. This construct was then introduced into the *PHBmu-GFP* reporter line. The resulting line (hereafter *indMIR165Amu/PHBmu-GFP*) was capable of ground tissue-specific and steroid hormone-inducible expression of miR165mu and tdTomatoEr, allowing us to analyze quantitatively the effects of ground tissue-derived miR165mu on the expression of *PHBmu-GFP*.

When *indMIR165Amu/PHBmu-GFP* plants were germinated in the presence of different concentrations of the inducer dexamethasone (DEX), expression of *PHBmu-GFP* was suppressed in the stele to a variable extent (Fig. 5C-E). This effect was caused by the sequence-specific suppressive function of miR165mu toward PHBmu-GFP, as control plants (*indMIR165Awt/PHBmu-GFP*) in which wild-type miR165 was expressed in the same manner did not affect the *PHBmu-GFP* expression pattern (Fig. 5F). We measured the fluorescence intensity of PHBmu:GFP in the peripheral and central stele, as well as the intensity of tdTomatoEr in the endodermis, which reflects the *MIR165Amu* transcription level (see Fig. S8 in the supplementary material). The intensity of PHBmu:GFP in the peripheral stele correlated inversely with the intensity of tdTomatoEr in the endodermis (r=0.70; s.d.=15.8), suggesting that endodermis-derived miR165mu suppressed the *PHBmu-GFP* level in the stele in a dose-dependent manner (Fig. 5A).

We then classified these roots into three categories based on their PHBmu:GFP expression pattern. Plants in category 1 showed PHBmu:GFP fluorescence throughout the root and the plants of this category were exclusively found among those grown without DEX (Fig. 5C). Plants in category 2 showed a PHBmu:GFP pattern similar to that observed for *PHB-GFP* in *scr-3* and *shr-2* backgrounds, with GFP expanded to the outermost stele but no further (Fig. 5D, compare with Fig. 4D,F). Plants in category 3 showed PHBmu:GFP only in the central stele, similar to the *PHB-GFP* and *PHBmu-GFP/MIR165Amu* roots (Fig. 5E, compare with Fig. 4B,E). We also analyzed the xylem differentiation status of each plant and found that most of the plants in categories 1 and 2 (92%, n=12) had metaxylem in the peripheral stele (Fig. 5G,H), whereas those in category 3 (89%, n=19) had protoxylem in the peripheral stele (Fig. 5I). Expression of *AHP6* and *SKOR*, as well as the capacity of the pericycle to form lateral root primordia, were also restored by inducing miR165mu, although lateral root primordium development was slightly retarded as compared with wild type (see Fig. S9B-D in the supplementary material) (Malamy and Benfey, 1997), indicating that miR165-dependent formation of the PHB expression gradient is required for pericycle function.

A comparison of the ratio of PHBmu:GFP intensities between the central and peripheral stele with the intensity of tdTomatoEr in the endodermis (Fig. 5B) revealed that the PHBmu:GFP ratio increases with increasing levels of *MIR165Amu* transcription in the endodermis, up to the miR165mu expression level roughly corresponding to ~50 units of tdTomatoER fluorescence intensity (horizontal axis in Fig. 5B) that was used to estimate transcriptional activation by GVG. This suggests that the level of *MIR165Amu* transcription in the endodermis has a quantitative effect on the formation of the PHBmu:GFP gradient in the stele. Taken together, these results suggest that, in wild-type roots, a certain level of *MIR165/166* transcription in the endodermis allows *PHB* expression to form a gradient across the stele, which is required for the correct arrangement of two xylem cell types and for pericycle differentiation.

miRNA-mediated regulation from the outer cell layer is crucial for the formation of the PHB gradient

The ability of the ground tissue-derived miR165mu to form a graded PHBmu:GFP distribution in the stele suggests that, in wild-type roots, endodermis-derived miR165 forms an activity gradient that decreases toward the central stele and thereby confers an inverse gradient of *PHB* transcripts across the stele. As a prerequisite to construct such a model, it is necessary to determine whether the ectopic production of miR165 within the stele efficiently suppresses *PHB* transcripts throughout the stele. It has been reported that transcription of *MIR165A* from the stele-specific *CYTOKININ RESPONSE 1* (*CRE1*) promoter (*pCRE1-MIR165A*) results in ectopic protoxylem formation in the central stele and reduced *PHB* expression levels (Carlsbecker et al., 2010). The expression pattern of *PHB* in the *pCRE1-MIR165A* roots, however, has not been analyzed.

We crossed *pCRE1-MIR165A* and *PHB-GFP* plants and found that the graded distribution of PHB:GFP was abolished in the stele of F1 plants, with very weak PHB:GFP fluorescence distributed in a broad domain in the stele (Fig. 6A). As reported previously, these roots have ectopic protoxylem in the central stele (Fig. 6C) (Carlsbecker et al., 2010). By contrast, when *pCRE1-MIR165A* was crossed with plants homozygous for both *PHBmu-GFP* and

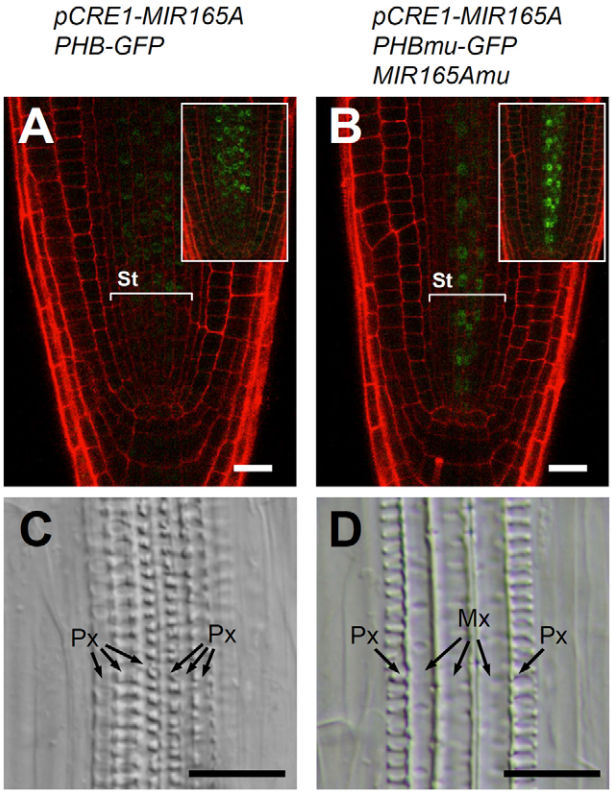

Fig. 6. Ectopic transcription of *MIR165A* in the stele abolishes the PHB expression gradient and metaxylem differentiation. (**A**,**C**) Production of miR165 specifically within the stele by *pCRE1-MIR165A* abolishes the graded distribution of PHB:GFP (A) and metaxylem differentiation (C). (**B**,**D**) *pCRE1-MIR165A* does not affect the PHBmu:GFP gradient formed with the aid of *MIR165Amu* (B), nor metaxylem differentiation (D). Insets (A,B) show images after threefold enhancement of the GFP signal. Scale bars: 10 μm.

MIR165Amu, the graded distribution of miR165-resistant (and functional) PHBmu:GFP was maintained in the stele (Fig. 6B). Concomitantly, these roots restored the normal xylem arrangement even in the presence of *pCRE1-MIR165A* (Fig. 6D), indicating that the PHB expression gradient alone is sufficient for correct xylem patterning. Taken together, these results suggest that the miR165/166-mediated suppression from the outer cell layer is crucial for the formation of the PHB expression gradient and hence for correct xylem patterning in the stele.

DISCUSSION

By restoring *MIR165A* transcription in the ground tissue of *shr* and *scr* using heterologous promoters, Carlsbecker et al. demonstrated that miR165 produced in the ground tissue non-cell-autonomously restricts *PHB* expression to the central stele (Carlsbecker et al., 2010). This experiment, however, did not address quantitative effects of miRNA on the spatial expression pattern of *PHB* in the stele. To visualize the expression pattern of *PHB* in relation to various levels of miR165/166 expression in the ground tissue, we generated two reporter lines, *PHB-GFP* and *PHBmu-GFP*, which faithfully recapitulated the distribution patterns and morphological phenotypes of endogenous *PHB* transcripts and its miR-insensitive mutant form, respectively (Fig. 4 and see Fig. S7 in the supplementary material). Consistent with the reduced miR165/166 levels in *shr* and *scr* mutants, *PHB-GFP* expression in *shr* and *scr* was moderately expanded as compared with that in wild type. In situ hybridization revealed similar expansion of endogenous *PHB* expression in *scr*. Furthermore, introduction of the *MIR165Amu* transgene, which targets the *PHBmu-GFP* transcripts, restricted *PHBmu-GFP* expression to the central stele, making it indistinguishable from that of *PHB-GFP* in wild type. Concomitantly, *MIR165Amu* suppressed most, if not all, of the *phb-1d*-like phenotype of *PHBmu-GFP* plants. These results indicate that the *PHBmu-GFP* and *MIR165Amu* transgenes closely mimic the relationship between the endogenous *PHB* and *MIR165A* genes. Therefore, plants harboring these transgenes provide a reliable tool for correlating the level of miRNA production in the ground tissue to the *PHB* expression pattern and xylem differentiation phenotype in the stele, under the conditions in which the effects of endogenous miR165/166 can be excluded.

We modified this system to explore the quantitative effects of miR165mu produced in the ground tissue, by placing *MIR165Amu* transcription under the ground tissue-specific and DEX-dependent transactivation system. The results indicated that the level of miR165mu in the ground tissue has a dose-dependent effect on the *PHB* expression pattern and on xylem cell type specification in the stele (Fig. 5). Production of miR165 within the stele abolished the PHB expression gradient (Fig. 6), providing developmental significance to the non-cell-autonomous regulation of *PHB* by miR165. These results strongly suggest that endogenous miR165 (and possibly miR166 as well) expressed in the endodermis can move towards the central stele, forming an activity gradient that decreases toward the central stele. Such an miR165/166 activity gradient is then translated into an inverse gradient of *PHB* transcripts across the stele (Fig. 7A). The *PHB* gradient thus formed specifies xylem cell types in a concentration-dependent manner, with a high dosage specifying metaxylem and a low dosage protoxylem (Fig. 7A) (Carlsbecker et al., 2010). This model explains the *PHB* expression patterns and cell differentiation defects observed in *scr*, *shr* and *phb-1d* mutants (Fig. 7B,C).

In wild-type roots, the distribution of *PHB* transcripts in the stele is somewhat biased toward the xylem pole (Fig. 4G), whereas transcription of either *PHB* or *MIR165/166* does not exhibit this

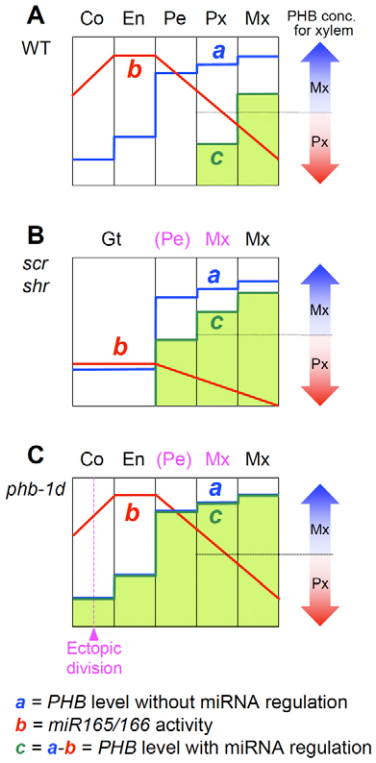

Fig. 7. Model of *PHB* suppression by the miR165/166 activity gradient and its outcome in the root radial pattern. The differentiation status of each cell file is shown at the top, with those altered by ectopic PHB expression in pink. Bidirectional arrows represent conceptual PHB concentration ranges that specify the two xylem cell types. (**A**) In the wild type, PHB expression is restricted to the central stele by the action of endodermis-derived miR165/166. (**B**) In *scr* and *shr*, attenuation of endodermis-derived miR165/166 activity results in elevated PHB expression throughout the stele, which in turn affects differentiation at the peripheral stele. (**C**) In *phb-1d*, the PHB expression domain expands further towards the ground tissue to affect its pattern formation.

bias (see Fig. S3J-L and Fig. S5 in the supplementary material). This suggests the existence of as yet unknown mechanisms that modulate the effect of miR165 within the stele. It has been reported that *ATHB8* and *CNA*, two of the HD-ZIP III genes targeted by miR165/166, are preferentially transcribed along the xylem pole (Lee et al., 2006; Carlsbecker et al., 2010). In these cells, less miR165/166 might be available for *PHB* suppression. Other mechanisms, such as differential miRNA mobility and/or the distribution of RNA-induced silencing complex (RISC) activity, are also conceivable.

In animal development, a signaling molecule emitted from a localized source confers differential gene expression along the field of its gradient thereby specifying different cell fates (Ashe and Briscoe, 2006). If the concentration of such a molecule is directly interpreted by an individual cell without relaying it to a second intercellular signal, the molecule is called a morphogen (Wolpert, 1969; Tabata and Takei, 2004). The mode of miR165/166 action revealed in our study and that of Carlsbecker et al. (Carlsbecker et al., 2010), i.e. they are emitted from a local source, affect neighboring tissues and their dosage is interpreted by each recipient cell for different cell fates, suggests the possibility that miR165/166 act as a novel morphogen. The mode of miR165/166 action,

however, is different from that of classical morphogens in that miR165/166 activity is first converted into an inverse gradient of HD-ZIP III levels. Since this conversion takes place in each recipient cell, this difference does not exclude miR165/166 from being considered morphogens. However, it is not clear whether miR165/166 form a concentration gradient across the stele, as is expected for a morphogen system. In situ hybridization for miR166 showed strong staining in the epidermis and cortex, whereas weak and apparently uniform staining was observed in the stele, suggesting that miR165/166 do not accumulate in the stele, where they are presumed to be consumed for *PHB* suppression (Carlsbecker et al., 2010). Therefore, although our study strongly suggests the presence of an miRNA activity gradient, its concentration gradient remains elusive or might even not exist.

In leaf development, trans-acting small interfering RNA (ta-siRNA) has been proposed to move from the abaxial-most cell layers, the site of its biogenesis, towards the internal tissue, forming an accumulation gradient along the adaxial-abaxial axis (Chitwood et al., 2009). In this case, however, the ta-siRNA gradient appears to sharpen the expression boundary of target transcripts rather than to form an inverse gradient. In a mathematical model, alteration of the parameters for miRNA diffusion rate and strength of miRNA-mRNA interaction affects the steepness of the mRNA gradient (Levine et al., 2007). This suggests that the effects of non-cell-autonomous small RNAs on the spatial expression patterns of their target transcripts should be analyzed experimentally on a case-by-case basis.

Our results revealed that miRNA-dependent suppression of *PHB* is also required for correct ground tissue patterning and pericycle differentiation (Figs 2, 3 and see Fig. S7 in the supplementary material). At least in the case of ground tissue, the observed defect was due to the ectopic expression of PHB in these cell layers and not to an indirect effect from the defective stele, as targeted expression of functional PHBmu:GFP protein in the ground tissue resulted in the same patterning defects (see Fig. S6 in the supplementary material). The presence of supernumerary ground tissue layers in *phb-1d* is consistent with the ectopic expression of SHR and SCR proteins in these cells (Fig. 2C-F) (Nakajima et al., 2001) and the downregulation of *JKD* in the *phb-1d* ground tissue (Fig. 2H,J). JKD prevents SHR protein movement and *SCR* transcription from expanding towards the cortex (Welch et al., 2007). Therefore, currently available data suggest a mechanism in which miRNA165/166 eliminate PHB expression from the ground tissue and maintain *JKD* expression, ensuring sequestration of SHR and SCR within the endodermis, which in turn is necessary for correct ground tissue patterning. The relatively low penetrance of the ground tissue defects might not be due to residual JKD in the *phb-1d* endodermis, as loss-of-function *jkd* mutants also show subtle defects in the ground tissue, possibly owing to functional redundancy with homologous genes (Welch et al., 2007).

In wild-type roots, *PHB* expression seems to be completely suppressed in the ground tissue, and hence it is not clear why *PHB* is transcribed there. It has been postulated that one of the developmental roles of miRNA-dependent regulation is to clear out key regulatory transcripts from daughter cell lineages (Rhoades et al., 2002). However, there is no known developmental function for PHB in the ground tissue lineage. An alternative explanation is that transcription of *PHB* is not regulated by tissue-specific factors in the *Arabidopsis* root, but instead depends on as yet unknown positional cues that emanate from the stele. A similar mechanism has been proposed for HD-ZIP III expression in the shoot (Emery et al., 2003).

Acknowledgements
We thank Philip Benfey, Yka Helariutta and Ji-Young Lee for critically reading the manuscript and supplying materials; Miyoko Morita-Terao, Jim Haseloff, Roger Tsien, Annelie Carlsbecker, Minoru Kubo, Noriyoshi Yagi and the Arabidopsis Biological Resource Center for technical advice and materials; and Mikio Nishimura, Makoto Hayashi and Mitsue Fukazawa at the National Institute for Basic Biology, Japan, for assistance with the microarray analysis. This work was supported in part by Grants-in-Aid for Scientific Research from the Japan Society for the Promotion of Science (JSPS) to K.N. (21027025) and S.M. (19-11231). S.M. and S.K. were supported by JSPS Research Fellowships for Young Scientists.

Competing interests statement
The authors declare no competing financial interests.

Supplementary material
Supplementary material for this article is available at
http://dev.biologists.org/lookup/suppl/doi:10.1242/dev.060491/-/DC1

References
Aoyama, T. and Chua, N. H. (1997). A glucocorticoid-mediated transcriptional induction system in transgenic plants. *Plant J.* **11**, 605-612.
Ashe, H. L. and Briscoe, J. (2006). The interpretation of morphogen gradients. *Development* **133**, 385-394.
Becker, D. (1990). Binary vectors which allow the exchange of plant selectable markers and reporter genes. *Nucleic Acids Res.* **18**, 203.
Bhalerao, R. P. and Bennett, M. J. (2003). The case for morphogens in plants. *Nat. Cell Biol.* **5**, 939-943.
Birnbaum, K., Shasha, D. E., Wang, J. Y., Jung, J. W., Lambert, G. M., Galbraith, D. W. and Benfey, P. N. (2003). A gene expression map of the Arabidopsis root. *Science* **302**, 1956-1960.
Carlsbecker, A. and Helariutta, Y. (2005). Phloem and xylem specification: pieces of the puzzle emerge. *Curr. Opin. Plant Biol.* **8**, 512-517.
Carlsbecker, A., Lee, J. Y., Roberts, C. J., Dettmer, J., Lehesranta, S., Zhou, J., Lindgren, O., Moreno-Risueno, M. A., Vaten, A., Thitamadee, S. et al. (2010). Cell signalling by microRNA165/6 directs gene dose-dependent root cell fate. *Nature* **465**, 316-321.
Chitwood, D. H., Nogueira, F. T., Howell, M. D., Montgomery, T. A., Carrington, J. C. and Timmermans, M. C. (2009). Pattern formation via small RNA mobility. *Genes Dev.* **23**, 549-554.
Clough, S. J. and Bent, A. F. (1998). Floral dip: a simplified method for Agrobacterium-mediated transformation of Arabidopsis thaliana. *Plant J.* **16**, 735-743.
Cui, H., Levesque, M. P., Vernoux, T., Jung, J. W., Paquette, A. J., Gallagher, K. L., Wang, J. Y., Blilou, I., Scheres, B. and Benfey, P. N. (2007). An evolutionarily conserved mechanism delimiting SHR movement defines a single layer of endodermis in plants. *Science* **316**, 421-425.
Dolan, L., Janmaat, K., Willemsen, V., Linstead, P., Poethig, S., Roberts, K. and Scheres, B. (1993). Cellular organisation of the Arabidopsis thaliana root. *Development* **119**, 71-84.
Emery, J. F., Floyd, S. K., Alvarez, J., Eshed, Y., Hawker, N. P., Izhaki, A., Baum, S. F. and Bowman, J. L. (2003). Radial patterning of Arabidopsis shoots by Class III HD-ZIP and KANADI genes. *Curr. Biol.* **13**, 1768-1774.
Fukaki, H. and Tasaka, M. (2009). Hormone interactions during lateral root formation. *Plant Mol. Biol.* **69**, 437-449.
Fukaki, H., Wysocka-Diller, J., Kato, T., Fujisawa, H., Benfey, P. N. and Tasaka, M. (1998). Genetic evidence that the endodermis is essential for shoot gravitropism in Arabidopsis thaliana. *Plant J.* **14**, 425-430.
Gallagher, K. L., Paquette, A. J., Nakajima, K. and Benfey, P. N. (2004). Mechanisms regulating SHORT-ROOT intercellular movement. *Curr. Biol.* **14**, 1847-1851.
Gaymard, F., Pilot, G., Lacombe, B., Bouchez, D., Bruneau, D., Boucherez, J., Michaux-Ferriere, N., Thibaud, J. B. and Sentenac, H. (1998). Identification and disruption of a plant shaker-like outward channel involved in K^+ release into the xylem sap. *Cell* **94**, 647-655.
Hara, K., Kajita, R., Torii, K. U., Bergmann, D. C. and Kakimoto, T. (2007). The secretory peptide gene EPF1 enforces the stomatal one-cell-spacing rule. *Genes Dev.* **21**, 1720-1725.
Helariutta, Y., Fukaki, H., Wysocka-Diller, J., Nakajima, K., Jung, J., Sena, G., Hauser, M.-T. and Benfey, P. N. (2000). The SHORT-ROOT gene controls radial patterning of the Arabidopsis root through radial signaling. *Cell* **101**, 555-567.
Himanen, K., Boucheron, E., Vanneste, S., de Almeida Engler, J., Inze, D. and Beeckman, T. (2002). Auxin-mediated cell cycle activation during early lateral root initiation. *Plant Cell* **14**, 2339-2351.
Hirakawa, Y., Shinohara, H., Kondo, Y., Inoue, A., Nakanomyo, I., Ogawa, M., Sawa, S., Ohashi-Ito, K., Matsubayashi, Y. and Fukuda, H. (2008). Non-cell-autonomous control of vascular stem cell fate by a CLE peptide/receptor system. *Proc. Natl. Acad. Sci. USA* **105**, 15208-15213.

Kondo, T., Kajita, R., Miyazaki, A., Hokoyama, M., Nakamura-Miura, T., Mizuno, S., Masuda, Y., Irie, K., Tanaka, Y., Takada, S. et al. (2010). Stomatal density is controlled by a mesophyll-derived signaling molecule. *Plant Cell Physiol.* **51**, 1-8.
Kouchi, H. and Hata, S. (1993). Isolation and characterization of novel nodulin cDNAs representing genes expressed at early stages of soybean nodule development. *Mol. Gen. Genet.* **238**, 106-119.
Kubo, M., Udagawa, M., Nishikubo, N., Horiguchi, G., Yamaguchi, M., Ito, J., Mimura, T., Fukuda, H. and Demura, T. (2005). Transcription switches for protoxylem and metaxylem vessel formation. *Genes Dev.* **19**, 1855-1860.
Kurata, T., Okada, K. and Wada, T. (2005). Intercellular movement of transcription factors. *Curr. Opin. Plant Biol.* **8**, 600-605.
Lee, J.-Y., Colinas, J., Wang, J. Y., Mace, D., Ohler, U. and Benfey, P. N. (2006). Transcriptional and posttranscriptional regulation of transcription factor expression in Arabidopsis roots. *Proc. Natl. Acad. Sci. USA* **103**, 6055-6060.
Levesque, M. P., Vernoux, T., Busch, W., Cui, H., Wang, J. Y., Blilou, I., Hassan, H., Nakajima, K., Matsumoto, N., Lohmann, J. U. et al. (2006). Whole-genome analysis of the SHORT-ROOT developmental pathway in Arabidopsis. *PLoS Biol.* **4**, e143.
Levine, E., McHale, P. and Levine, H. (2007). Small regulatory RNAs may sharpen spatial expression patterns. *PLoS Comp. Biol.* **3**, e233.
Liu, Y. G., Mitsukawa, N., Oosumi, T. and Whittier, R. F. (1995). Efficient isolation and mapping of Arabidopsis thaliana T-DNA insert junctions by thermal asymmetric interlaced PCR. *Plant J.* **8**, 457-463.
Lloyd, A. M., Schena, M., Walbot, V. and Davis, R. W. (1994). Epidermal cell fate determination in Arabidopsis: patterns defined by a steroid-inducible regulator. *Science* **266**, 436-439.
Mähönen, A. P., Bishopp, A., Higuchi, M., Nieminen, K. M., Kinoshita, K., Tormakangas, K., Ikeda, Y., Oka, A., Kakimoto, T. and Helariutta, Y. (2006). Cytokinin signaling and its inhibitor AHP6 regulate cell fate during vascular development. *Science* **311**, 94-98.
Malamy, J. E. and Benfey, P. N. (1997). Organization and cell differentiation in lateral roots of *Arabidopsis thaliana*. *Development* **124**, 33-44.
Mallory, A. C., Reinhart, B. J., Jones-Rhoades, M. W., Tang, G., Zamore, P. D., Barton, M. K. and Bartel, D. P. (2004). MicroRNA control of PHABULOSA in leaf development: importance of pairing to the microRNA 5′ region. *EMBO J.* **23**, 3356-3364.
Matsuzaki, Y., Ogawa-Ohnishi, M., Mori, A. and Matsubayashi, Y. (2010). Secreted peptide signals required for maintenance of root stem cell niche in Arabidopsis. *Science* **329**, 1065-1067.
McConnell, J. and Barton, M. (1998). Leaf polarity and meristem formation in Arabidopsis. *Development* **125**, 2935-2942.
McConnell, J. R., Emery, J., Eshed, Y., Bao, N., Bowman, J. and Barton, M. K. (2001). Role of PHABULOSA and PHAVOLUTA in determining radial patterning in shoots. *Nature* **411**, 709-713.
Miyashima, S., Hashimoto, T. and Nakajima, K. (2009). ARGONAUTE1 acts in Arabidopsis root radial pattern formation independently of the SHR/SCR pathway. *Plant Cell Physiol.* **50**, 626-634.
Morita, M. T., Kato, T., Nagafusa, K., Saito, C., Ueda, T., Nakano, A. and Tasaka, M. (2002). Involvement of the vacuoles of the endodermis in the early process of shoot gravitropism in Arabidopsis. *Plant Cell* **14**, 47-56.
Nakajima, K., Sena, G., Nawy, T. and Benfey, P. N. (2001). Intercellular movement of the putative transcription factor SHR in root patterning. *Nature* **413**, 307-311.
Ochando, I., Gonzalez-Reig, S., Ripoll, J. J., Vera, A. and Martinez-Laborda, A. (2008). Alteration of the shoot radial pattern in Arabidopsis thaliana by a gain-of-function allele of the class III HD-Zip gene INCURVATA4. *Int. J. Dev. Biol.* **52**, 953-961.
Paquette, A. J. and Benfey, P. N. (2005). Maturation of the ground tissue of the root is regulated by gibberellin and SCARECROW and requires SHORT-ROOT. *Plant Physiol.* **138**, 636-640.
Prigge, M. J., Otsuga, D., Alonso, J. M., Ecker, J. R., Drews, G. N. and Clark, S. E. (2005). Class III homeodomain-leucine zipper gene family members have overlapping, antagonistic, and distinct roles in Arabidopsis development. *Plant Cell* **17**, 61-76.
Reinhart, B. J., Weinstein, E. G., Rhoades, M. W., Bartel, B. and Bartel, D. P. (2002). MicroRNAs in plants. *Genes Dev.* **16**, 1616-1626.
Rhoades, M. W., Reinhart, B. J., Lim, L. P., Burge, C. B., Bartel, B. and Bartel, D. P. (2002). Prediction of plant microRNA targets. *Cell* **110**, 513-520.
Sena, G., Jung, J. W. and Benfey, P. N. (2004). A broad competence to respond to SHORT ROOT revealed by tissue-specific ectopic expression. *Development* **131**, 2817-2826.
Shaner, N. C., Campbell, R. E., Steinbach, P. A., Giepmans, B. N., Palmer, A. E. and Tsien, R. Y. (2004). Improved monomeric red, orange and yellow fluorescent proteins derived from Discosoma sp. red fluorescent protein. *Nat. Biotechnol.* **22**, 1567-1572.
Stahl, Y., Wink, R. H., Ingram, G. C. and Simon, R. (2009). A signaling module controlling the stem cell niche in Arabidopsis root meristems. *Curr. Biol.* **19**, 909-914.
Sugano, S. S., Shimada, T., Imai, Y., Okawa, K., Tamai, A., Mori, M. and Hara-Nishimura, I. (2010). Stomagen positively regulates stomatal density in Arabidopsis. *Nature* **463**, 241-244.
Tabata, T. and Takei, Y. (2004). Morphogens, their identification and regulation. *Development* **131**, 703-712.
Tang, F., Hajkova, P., Barton, S. C., Lao, K. and Surani, M. A. (2006). MicroRNA expression profiling of single whole embryonic stem cells. *Nucleic Acids Res.* **34**, e9.
Tang, G., Reinhart, B. J., Bartel, D. P. and Zamore, P. D. (2003). A biochemical framework for RNA silencing in plants. *Genes Dev.* **17**, 49-63.
Welch, D., Hassan, H., Blilou, I., Immink, R., Heidstra, R. and Scheres, B. (2007). Arabidopsis JACKDAW and MAGPIE zinc finger proteins delimit asymmetric cell division and stabilize tissue boundaries by restricting SHORT-ROOT action. *Genes Dev.* **21**, 2196-2204.
Wolpert, L. (1969). Positional information and the spatial pattern of cellular differentiation. *J. Theor. Biol.* **25**, 1-47.

Table S1. Primers

Name	Sequence (5′ to 3′)
For qRT-PCR	
miR165UPL (for pulsed RT)	GTTGGCTCTGGTGCAGGGTCCGAGGTATTCGCACCAGAGCCAACGGGGGA
miR165/166f	TCGCTTCGGACCAGGCTTCA
miR165/166r	GTGCAGGGTCCGAGGT
pri-miR165mu-f	ATAGAGAGTATCCTCGGTCCT
pri-miR165mu-r	TGATAATCATCGCAAGACCG (complementary to NosT)
JKDf	GCGAAAACTTGTGGTACTCGT
JKDr	CGCAGAACGCTCTATGTGTG
SKORf	CCGTCATTAATGGAATCAGAGA
SKORr	TCGTCCACGCCTTGTACC
tdTomatoEr-f	CTGTTCCTGTACGGCATGG
tdTomatoEr-r	GGGGAAATTCGAGCTATGGT
ACT7f	CGCTGCTTCTCGAATCTTCT
ACT7r	CCATTCCAGTTCCATTGTCA
AHP6f	ATATCTGACTCCTGCAGCT
AHP6r	TTGAGAGGACTGGAGGTAGT
PHBf	TTGGTTTCAGAACCGCAGA
PHBr	CTGTTTGAAGACGAGCAGCTT
PHVf	TGCAGCAGGGATATGCGAATCTTC
PHVr	ACCGTCGCTTGCTCAT ACGAAAC
REVf	CGCCAAGCTAATGCAACAGGGATT
REVr	TGTCTTCCCATCGTTGACACACAG
For DNA construction	
PHB-GFP construction	
Xba-PHB-(–)3570	ACTCTAGACGTTTGTAGACTCTAGTC
Kpn-PHB-(+)5015R	ACGGTACCAGCTAGCTCATTCATCTATCT
PHB(+)miR1445F	CCTGGaCCaGATTCTATTGGCA
PHB(+)miR1444R	CTACACCAGCAATGAAGG
HpaI-PHBCterF	GTTAACTGAAGAATAATAAGAAATAAGAAG
PHB(+)4443R	AACGAACGACCAATTCACGAACA
PHB(–)287	CTGTCGACTTCGCTTCTCCTTCCTCTCC
PHB-4546R	CAACTAGTTTTGGAGCATAGTGGCACC
PHB in situ probe	
PHB-2642	CTTTGGTAGTGGCGTGCTTT
PHB-4085c	AATGTGAAAACCGGTGAAGC
MIR165/166 promoters	
MIR165A(–)3927	GTATCCTAGCGAAGTAGATTCG
MIR165A-ProEND	TCAACTGAAATAGCTTAACCCTC
MIR165B(–)2561	GAGTCGACATGGGGTTTAGACAGTGGC
MIR165B-ProEND	CAGGATCCACAACAGAAATAGCCTCTTCATGATTATC
MIR166A(–)3132	CTGTCGACCGGACACAACACAAAACACAACTC
MIR166A-ProEND	CAGGATCCTCAAAAGAGAAAGCCCCTTTTTCTT
MIR166B(–)3022	TAGTCGACTGAGTTTGGAATCTGAGACG
MIR166B-ProEND	CAGGATCCTCAAAAGAAAAATCCCTCTTTAAATCC
MIR166C(–)798	TCGTCGACTGGCTCTAGTCAACATTTTCAC
MIR166C-ProEND	CAGGATCCTCAACACTAAATCGCACAACAATG
MIR166D(–)1873	GCGTCGACCCCCCTAACCTACTTATCGC
MIR166D-ProEND	TAGGATCCTCAACCCTAAACCAAAGCAGGATAAC
MIR166E(–)1649	AGGTCGACGGCTCAAGAGACTCGTAACC
MIR166E-ProEND	CAGGATCCTCAAAAGGAAAAGCTTCACTGAAG
MIR166F(–)1027	TAGTCGACTGCAAACCCTCTTTCTCATCC
MIR166F-ProEND	CAGGATCCTGAACTTTTGGCTCAGAAAGACAGAG
MIR166G(–)2223	TAGTCGACGCAAGATGAAGAAGAAACAGAGAG
MIR166G-ProEND	CAGGATCCTAAACCCTAAATCGCTTCACTATAAG
MIR165A expression constructs	
MIR165A(+)722R	GGCCACGTCATTTTCTATCC
MIR165A(+)93mu	GAGAGTATCCTCGGtCCtGGCTT
MIR165A(+)70R	TATGATCACTTGAATCATTAAC
Hind-MIR165A(–)33	GCAAGCTTCGATTATCATGAGGGTTAAG
Bam-MIR165A(+)135R	AAGGATCCAATAAATGGTGATCAGAGGCA
SKOR promoter	
SKOR(–)1842	TGAAGCTTGAGCTCAACATCTTTGAATAAAC
SKOR-ProEnd	CCGGATCCTACACCTCCGAATCACGATACCAG
JKD promoter	
Bam-JKD (–)3603	TTGGATCCTAGCAAGTGGAACTAGAAGCG
JKD-ProEnd	ATCTGTGTTTTAATTTAAAACGGATCGG
J0571 promoter	
J0571-up	CCAAGTGAAAGCTTAGAAAGCAG
GAL4VP16-3	CGATGGAGGACAGGAGCTTCATTG

Underline indicates introduced restriction site.
Lowercase indicates mutations introduced into *PHB* and *MIR165A*.

Table S2. Genes downregulated in *scr-3* and enriched in the root stele

Gene ID	Fold decrease in *scr-3*	Fold enrichment in the stele*	TAIR8 annotation	Reference†
At2g18800	24.89	5.90	Xyloglucan:xyloglucosyl transferase, putative, AtXTH21	Liu et al., 2007
At1g73220	21.16	3.46	ARABIDOPSIS THALIANA ORGANIC CATION/CARNITINE TRANSPORTER 1 (ATOCT1)	Lelandais-Briere et al., 2007
At2g39510	18.61	4.05	Nodulin MtN21 family protein	–
At1g80100	17.72	5.64	AHP6, ARABIDOPSIS HISTIDINE PHOSPHOTRANSFER PROTEIN 6 (AHP6)	Mähönen et al., 2006
At3g26610	17.60	3.66	Polygalacturonase, putative	–
At4g30450	14.42	4.33	Glycine-rich protein	–
At3g53980	14.21	4.34	Protease inhibitor/seed storage/lipid transfer protein (LTP) family protein	Wenzel et al., 2008
At5g10580	12.61	3.31	Unknown protein	–
At4g33550	12.19	3.06	Protease inhibitor/seed storage/lipid transfer protein (LTP) family protein	–
At4g20210	12.09	10.37	Terpene synthase/cyclase family protein	–
At3g02850	11.24	3.18	Stelar K^+ outward rectifying channel (SKOR)	Gaymard et al., 1998
At1g78090	11.12	5.38	TREHALOSE-6-PHOSPHATE PHOSPHATASE	–
At3g62040	10.17	3.42	Similar to haloacid dehalogenase-like hydrolase family protein	–
At5g25840	9.37	5.37	Unknown protein	–
At3g13810	8.58	5.77	Unknown protein	–
At4g36740	8.08	6.69	ARABIDOPSIS THALIANA HOMEOBOX PROTEIN 40 (ATHB40)	–
At1g01070	6.72	9.03	Nodulin MtN21 family protein	–
At1g67710	6.19	3.41	ARABIDOPSIS RESPONSE REGULATOR 11 (ARR11)	Tajima et al., 2004
At1g44800	5.85	6.88	Nodulin MtN21 family protein	–
At3g25190	5.42	4.63	Nodulin, putative	–
At4g11310	4.66	6.94	Cysteine proteinase precursor-like protein	–
At4g01450	4.45	4.34	Nodulin MtN21 family protein	–
At4g30460	4.28	3.23	Glycine-rich protein	Ko et al., 2006
At3g45700	4.27	7.33	Proton-dependent oligopeptide transport (POT) family protein	–
At3g49760	3.64	5.41	ARABIDOPSIS THALIANA BASIC LEUCINE-ZIPPER 5 (ATBZIP5)	Dinneny et al., 2008
At1g24530	3.55	3.07	Transducin family protein/WD-40 repeat family protein	–
At1g18140	3.40	6.17	LACCASE 1 (LAC1)	–
At5g06730	3.17	4.10	Peroxidase 54 precursor (PER54)	–
At2g21560	3.12	5.39	Unknown protein	–
At5g47450	3.10	3.42	TONOPLAST INTRINSIC PROTEIN 2;3 (ATTIP2;3)	–

*Fold enrichment in the stele was derived from the microarray data of Birnbaum et al. (Birnbaum et al., 2003) by the following calculation: expression in the stele (average of three developmental zones)/expression in the cell layer with the second highest expression (average of three developmental zones).

†References are shown only for those demonstrating expression and/or functions in the root stele.

References

Dinneny, J. R., Long, T. A., Wang, J. Y., Jung, J. W., Mace, D., Pointer, S., Barron, C., Brady, S. M., Schiefelbein, J. and Benfey, P. N. (2008). Cell identity mediates the response of Arabidopsis roots to abiotic stress. *Science* **320**, 942-945.

Ko, J. H., Beers, E. P. and Han, K. H. (2006). Global comparative transcriptome analysis identifies gene network regulating secondary xylem development in Arabidopsis thaliana. *Mol. Genet. Genomics* **276**, 517-531.

Lelandais-Briere, C., Jovanovic, M., Torres, G. A., Perrin, Y., Lemoine, R., Corre-Menguy, F. and Hartmann, C. (2007). Disruption of AtOCT1, an organic cation transporter gene, affects root development and carnitine-related responses in Arabidopsis. *Plant J.* **51**, 154-164.

Liu, Y. B., Lu, S. M., Zhang, J. F., Liu, S. and Lu, Y. T. (2007). A xyloglucan endotransglucosylase/hydrolase involved in growth of primary root and alters the deposition of cellulose in Arabidopsis. *Planta* **226**, 1547-1560.

Tajima, Y., Imamura, A., Kiba, T., Amano, Y., Yamashino, T. and Mizuno, T. (2004). Comparative studies on the type-B response regulators revealing their distinctive properties in the His-to-Asp phosphorelay signal transduction of Arabidopsis thaliana. *Plant Cell Physiol.* **45**, 28-39.

Wenzel, C. L., Hester, Q. and Mattsson, J. (2008). Identification of genes expressed in vascular tissues using NPA-induced vascular overgrowth in Arabidopsis. *Plant Cell Physiol.* **49**, 457-468.